LETTER

# Parameter-Dependent Superconducting Transition Temperature in a Sign-Problem-Free Bilayer Model

# Parameter-Dependent Superconducting Transition Temperature in a Sign-Problem-Free Bilayer Model

Runyu Ma[1], Zenghui Fan[1], Tianxing Ma[1,2*], and Congjun Wu[3,4,5,6*]

[1]*School of Physics and Astronomy, Beijing Normal University, Beijing 100875, China*
[2]*Key Laboratory of Multiscale Spin Physics(Ministry of Education), Beijing Normal University, Beijing 100875, China*
[3]*New Cornerstone Science Laboratory, Department of Physics, School of Science, Westlake University, Hangzhou 310024, China*
[4]*Institute for Theoretical Sciences, Westlake University, Hangzhou 310024, China*
[5]*Key Laboratory for Quantum Materials of Zhejiang Province, School of Science, Westlake University, Hangzhou 310024, China*
[6]*Institute of Natural Sciences, Westlake Institute for Advanced Study, Hangzhou 310024, China*

(Received 30 June 2025; accepted manuscript online 15 September 2025)

Recent discovery of high transition temperature superconductivity in $La_3Ni_2O_7$ has sparked renewed theoretical and experimental interests in unconventional superconductivity. It is crucial to understand the influence of various factors on its superconductivity. By refining the determinant quantum Monte Carlo algorithm, we characterize the parameter dependence of the superconducting transition temperature within a bilayer Hubbard model, which is sign-problem-free at arbitrary filling. A striking feature of this model is its similarity to the bilayer nickelate-based superconductor $La_3Ni_2O_7$, where superconductivity emerges from the bilayer $NiO_2$ planes. We find that interlayer spin-exchange $J$ is critical to interlayer pairing, and that on-site interaction $U$ contributes negatively to superconductivity at low doping levels but positively at high doping levels. Our findings can provide a reference for the next step in theoretical research on nickelate-based superconductors.

DOI: 10.1088/0256-307X/42/11/110705 CSTR: 32039.14.0256-307X.42.11.110705

*1. Introduction.* Since the discovery of unconventional superconductivity in doped cuprates,[1,2] understanding the parameter dependence of superconducting transition temperatures $T_c$ has been one of the most crucial and challenging tasks in condensed matter physics and materials science. Experimentally, researchers are continually seeking out new unconventional superconducting systems, hoping to discover those with even higher superconducting transition temperatures. After a few decades of intensive studies, a series of superconducting materials have been developed, including multilayer copper-based superconductors,[3–5] iron-based superconductors,[6–11] and the most recent discoveries of nickelate-based superconductors.[12,13] Theoretically, due to the effect of strong electronic correlation, characterizing the parameter-dependence of superconducting transition temperatures has proved to be especially difficult as not only is an effective microscopic model still lacking or uncertain but also its dependence has been shown to be exceptionally sensitive to small changes in model terms and parameters such as temperature, interaction, or doping. The Hubbard model or its extension is widely believed to be relevant to this problem and has motivated an enormous amount of work over the past six decades.[14] However, the relevant model parameters are in the most difficult regime where most approaches struggle; this remains the central model studied by theorists.[15–17] Recently, methods using the static-auxiliary-field approximation[18] have made great progress in explaining $T_c$ for major families of unconventional superconductors.[19,20] While unbiased methods for exact numerical values exist—some quantum Monte Carlo algorithms show superiority—but they run into the notorious sign problem especially in superconductivity which is greatly determined by the model.

Therefore, developing simplified models that permit exact numerical solutions provides a valuable computational platform to explore parameter-dependent trends in $T_c$ and identify generic mechanisms,[21–23] which complement analytical approaches. Among the numerous numerical methods, the determinant quantum Monte Carlo (DQMC) method aims to acquire exact numerical results without approximations; however, it is generally powerful for intermediate correlation regimes but suffers from a severe sign problem when heavily doped. Hence, establishing a minimal sign-problem-free model is a crucial aspect of DQMC studies. A promising candidate is a bilayer model with time-reversal-symmetric interactions following the Hubbard–Stratonovich (HS) transition.[24] In this context, the DQMC simulations of a sign-problem-free model, which includes on-site Hubbard interaction and interlayer spin-exchange,[25,26] offer unique advantages across extensive parameter regimes (i.e., all doping regimes), a fea-

*Corresponding authors. Email: txma@bnu.edu.cn; wucongjun@westlake.edu.cn

ture that is analogous to the nickelate-based material, $La_3Ni_2O_7$ (LNO). The strategy of designing sign-problem-free bilayer geometries has also been a crucial enabler for obtaining exact finite-temperature benchmarks of superconductivity in other contexts, such as cold-atom systems modeled by attractive Hubbard interactions.[27–29] While the full electronic structure of LNO requires multi-orbital descriptions, our minimal bilayer model captures the essential physical factors and isolates the proposed interlayer pairing mechanism for qualitative descriptions. Although minimal, this model offers a rare opportunity to explore superconductivity without methodological biases, advancing our understanding of generic mechanisms applicable to broader material classes.

Superconductivity in nickelate-based materials is first observed in the family of infinite-layer nickelate thin-film materials $A_{1-x}B_xNiO_2$ ($A$ = La, Nd, Pr, $B$ = Sr, Ca).[12,30–32] Soon afterwards, signatures of superconductivity in LNO were observed,[13] and its $T_c$ reaches 80 K under high pressure. In addition to its superconductivity, the magnetism and other properties of LNO have also been investigated.[33,34] From a theoretical point of view, the electronic properties of LNO are determined by the bilayer $NiO_2$ planes, considering $d_{x^2-y^2}$ and $d_{z^2}$ orbitals, which can capture most of the low-energy electronic structures;[35,36] these two orbitals are essentially associated with superconductivity in LNO. To explain the pairing mechanism of LNO, various interaction terms have been proposed to construct a promising model for LNO and describe its superconductivity. A possible mechanism is interlayer s-wave pairing induced by the interlayer spin-exchange of either $d_{x^2-y^2}$ or $d_{z^2}$ orbitals.[37–39] A relatively interesting argument is that the interlayer spin-exchange involving $d_{z^2}$ originates from strong interlayer hopping, and the interlayer spin-exchange of $d_{x^2-y^2}$ is passed from $d_{z^2}$ due to Hund's rule coupling or hybridization. Under large Hund's coupling, $d_{x^2-y^2}$ spins are forced to align with those of $d_{z^2}$; integrating out the $d_{z^2}$ degrees of freedom results in an effective interlayer spin-exchange within the $d_{x^2-y^2}$ orbital.[38,40] Consequently, a reduced Hamiltonian can be derived that represents a bilayer single-orbital model containing a large interlayer spin-exchange. Furthermore, in some other works, superconductivity in LNO is attributed to its similarity with doped cuprates.[41–43]

The promising low-energy reduced model of nickelate-based superconductors is quite similar to the sign-problem-free microscopic model sketched in Fig. 1(a), which provides a rare opportunity to study the parameter-dependent $T_c$ with exact numerical methods based on a realistic model closely related to real materials. In this work, we establish a computational framework to analyze key parameter-dependence of $T_c$ (i.e., on electron correlation and filling) in a minimal sign-problem-free bilayer model, using numerically exact DQMC simulations. We characterize $T_c$ by using the universal jump in the superfluid density over a broad range of electron filling $\langle n\rangle$ and coupling strength $U$. Interestingly, we find that $U$ benefits superconductivity at high doping levels and harms it

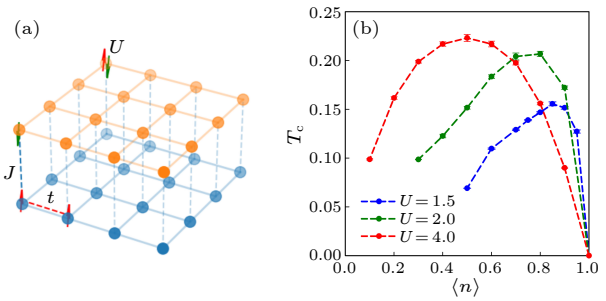


**Fig. 1.** (a) A sketch of the bilayer model used in this work, and periodic boundary condition is imposed in both directions. (b) The superconducting transition temperature $T_c$ as a function of electron filling $\langle n\rangle$ from $U = 1.5$ to $U = 4.0$.

at low doping levels, and we also find that $t_\perp$ inhibits superconductivity, which is summarized in Fig. 1(b). Furthermore, we demonstrate the regular part of resistivity $R^{\rm reg}$, which shows a strange-metal-like behavior, but the strange metallicity needs to be further confirmed. These results demonstrate the potential of this bilayer sign-free model in studies of LNO and superconductivity, and may also help to resolve the problem of the pairing mechanism in LNO.

*2. Model and Method.* The sign-problem-free microscopic model we used can be written as

$$\begin{aligned} H = & -t\sum_{\langle i,j\rangle}(\psi_i^\dagger\psi_j + \text{H.c.}) - \mu\sum_i n_i - t_\perp\sum_i \psi_i^\dagger \Gamma^4 \psi_i \\ & - \sum_{i,a=1-5}\frac{g_a}{2}(\psi_i^\dagger\Gamma^a\psi_i)^2 - \sum_i \frac{g_0}{2}(\psi_i^\dagger\psi_i - 2)^2, \end{aligned} \tag{1}$$

where we define $\psi_i = (c_{i1\uparrow}, c_{i1\downarrow}, c_{i2\uparrow}, c_{i2\downarrow})^{\rm T}$, $n_i = \psi_i^\dagger\psi_i$ and $c_{il\sigma}$ is the annihilation operator for an electron at site $i$, in layer $l$, with spin $\sigma$. The sign-problem-free nature of the model originates from the time-reversal symmetry ensured by the five $\Gamma$ matrices used here,[24,44]

$$\Gamma^{1-3} = \begin{pmatrix} \boldsymbol{\sigma} & 0 \\ 0 & -\boldsymbol{\sigma} \end{pmatrix}, \quad \Gamma^4 = \begin{pmatrix} 0 & I \\ I & 0 \end{pmatrix}, \quad \Gamma^5 = \begin{pmatrix} 0 & \mathrm{i}I \\ -\mathrm{i}I & 0 \end{pmatrix}, \tag{2}$$

which ensures the positive definiteness of the fermion determinant at any electron doping under specific parameter conditions.

For convenience, we rewrite the Hamiltonian Eq. (1) in the following form:

$$\begin{aligned} H = & -t\sum_{\langle i,j\rangle l\sigma}(c_{il\sigma}^\dagger c_{jl\sigma} + \text{H.c.}) - t_\perp\sum_{i\sigma}(c_{i1\sigma}^\dagger c_{i2\sigma} + \text{H.c.}) \\ & - \mu\sum_{il\sigma} n_{il\sigma} + U\sum_{il}\left(n_{il\uparrow} - \frac{1}{2}\right)\left(n_{il\downarrow} - \frac{1}{2}\right) \\ & + J_z\sum_i S_{i1}^z S_{i2}^z + \frac{J_\perp}{2}\sum_i (S_{i1}^+ S_{i2}^- + \text{H.c.}), \end{aligned} \tag{3}$$

where $S_{il}^z = \frac{1}{2}(n_{il\uparrow} - n_{il\downarrow})$, $S_{il}^+ = c_{il\uparrow}^\dagger c_{il\downarrow}$, and $n_{il\sigma} = c_{il\sigma}^\dagger c_{il\sigma}$. $S_{il}^-$ is the Hermitian conjugate of $S_{il}^+$, $U = g_1 + g_2 + g_3 - g_0$, $J_z = 4g_3 + 4g_0$, and $J_\perp = 2g_1 + 2g_2 + 4g_0$. We tune the chemical potential $\mu$ to achieve the desired electron filling $\langle n\rangle = 1/2L^2\langle\sum_{il\sigma} n_{il\sigma}\rangle$ per site (i.e., per orbital for all spins). Unless otherwise specified, $g_0$, $g_4$, and $g_5$ are set to 0 and $g_1 = g_2 = g_3$; this results in

$J_\perp = J_z = 4U/3$. We set $t = 1.0$ as the energy unit. An illustration of our model is shown in Fig. 1(a). To some extent, this model is similar to the bilayer nickelate model proposed in Refs. [37,38] and the mixed-dimensional (mixD) model proposed in Ref. [45], except that the spin-exchange in our model may be significantly large.

To investigate the properties of this model, we use the DQMC algorithm to compute the observables at finite temperature, $\langle O\rangle = \mathrm{Tr}\mathrm{e}^{-\beta H}O/\mathrm{Tr}\mathrm{e}^{-\beta H}$. In the DQMC algorithm, the $\mathrm{e}^{-\beta H}$ term is discretized into small time slices, $\mathrm{e}^{-\beta H} = \prod_M \mathrm{e}^{-\mathrm{d}\tau H}$, where $M\mathrm{d}\tau = \beta$. Here, we use a uniform and sufficiently small $\Delta\tau = 0.1$, so that the Trotter errors $\mathcal{O}(\Delta\tau^2)$ are smaller than those associated with the statistical sampling. Then the interaction part of the Hamiltonian is decoupled via HS transformation, $\mathrm{e}^{-\mathrm{d}\tau H} = \mathrm{e}^{-\mathrm{d}\tau H_0}\prod_{i,a=1\text{–}3}\sum_{l_{ia}}\gamma_{l_{ia}}\mathrm{e}^{\eta_{l_{ia}}\Gamma^a} = \sum_{\boldsymbol{l}=(l_1,l_2,\ldots)}\boldsymbol{B}(l)$. After that, the observables can be expressed as a sum over configurations of noninteracting systems. For more details on the DQMC algorithm, please see Refs. [46,47].

The sign problem occurs when the determinant $P(C)$ is not positive definite. The usual reweighting process makes the observables become $\frac{\sum_C \boldsymbol{P}(C)\boldsymbol{O}(C)/\sum|\boldsymbol{P}(C)|}{\sum\boldsymbol{P}(C)/\sum|\boldsymbol{P}(C)|}$. Defining $S(C) = \frac{\boldsymbol{P}(C)}{|\boldsymbol{P}(C)|}$, the expression becomes $\frac{\sum_C|\boldsymbol{P}(C)|S(C)\boldsymbol{O}(C)/\sum|\boldsymbol{P}(C)|}{\sum|\boldsymbol{P}(C)|S(C)/\sum|\boldsymbol{P}(C)|}$. Then common Monte Carlo sampling process can then be applied to both the denominator and the numerator. However, when the positive and negative terms of $P(C)$ nearly cancel, the denominator will have a large statistical error compared to its value. The accuracy of the simulations will be severely degraded. A special family of models ensures that $P(C)$ is positive; these models have a Kramers-symmetric interaction operator $V$. The model used in this work is one of this family. More details about these models can be found in Refs. [24,44].

*3. Results and Discussions.* Following previous works,[25] the superconducting order parameter is defined as

$$O_{\mathrm{SC}} = \frac{1}{\sqrt{2}}\sum_i(c_{i1\uparrow}c_{i2\downarrow} - c_{i1\downarrow}c_{i2\uparrow}). \tag{4}$$

To identify the superconducting transition temperature $T_\mathrm{c}$, we analyze the superfluid density $\rho_\mathrm{s}$, and we briefly describe the calculation of $\rho_\mathrm{s}$ below.[48,49]

First, we define the $x$ component of the current density operator

$$j_x(i,\tau) = \mathrm{e}^{\tau H}\left[\sum_{l=1,2}\sum_{\sigma=\uparrow,\downarrow} -\mathrm{i}c^\dagger_{i+xl\sigma}c_{il\sigma} + \mathrm{i}c^\dagger_{il\sigma}c_{i+xl\sigma}\right]\mathrm{e}^{-\tau H}, \tag{5}$$

and the corresponding response function is expressed as follows:

$$\Lambda_{xx}(\boldsymbol{q}) = \frac{1}{N_{\mathrm{site}}}\sum_{i,j}\int_0^\beta \mathrm{d}\tau\mathrm{e}^{\mathrm{i}\boldsymbol{q}\cdot(\boldsymbol{R}_i-\boldsymbol{R}_j)}\langle j_x(i,\tau)j_x(j,0)\rangle. \tag{6}$$

The superfluid density is the difference of the limiting longitudinal and transverse responses of current-current correlations,

$$\rho_\mathrm{s} = \frac{1}{4}(\Lambda^\mathrm{L} - \Lambda^\mathrm{T}), \tag{7}$$

where

$$\Lambda^\mathrm{L} = \lim_{q_x\to 0}\Lambda_{xx}(q_x, q_y = 0),$$
$$\Lambda^\mathrm{T} = \lim_{q_y\to 0}\Lambda_{xx}(q_x = 0, q_y). \tag{8}$$

At the Kosterlitz–Thouless (KT) transition, the universal-jump relation holds,[50,51]

$$T_\mathrm{c} = \frac{\pi}{2}\rho_\mathrm{s}^-. \tag{9}$$

Here $\rho_\mathrm{s}^-$ means the value of superfluid density below the critical temperature $T_\mathrm{c}$. To identify $T_\mathrm{c}$, we plot $\rho_\mathrm{s}(T)$ and find its intercept with $2T/\pi$.

From the calculated current-current correlations, one can deduce the regular part of optical resistivity readily,

$$R^{\mathrm{reg}} = \pi T^2\left[\frac{1}{N_{\mathrm{site}}}\sum_{i,j}\langle j_x(i,\beta/2)j_x(j,0)\rangle\right]^{-1}, \tag{10}$$

and this relation is applicable at relatively high temperatures.[52,53] Although this value may not be a faithful representation of DC transport, $R^{\mathrm{reg}}$ is helpful for further investigation, such as deducing the Drude weight.[54]

Besides, the superconducting susceptibility $\chi_{\mathrm{SC}}(\beta)$ is defined as

$$\chi_{\mathrm{SC}}(\beta) = \frac{1}{N_{\mathrm{site}}}\int_0^\beta \mathrm{d}\tau\sum_{i,j}\langle\mathrm{e}^{\tau H}O_{\mathrm{SC}}\mathrm{e}^{-\tau H}O_{\mathrm{SC}}\rangle. \tag{11}$$

For the KT transition, the superconducting susceptibility $\chi_{\mathrm{SC}}$ satisfies the scaling relation $\chi_{\mathrm{SC}} \sim L^{1.75}f(L/\xi)$, where $\xi \sim \exp(A/(T-T_\mathrm{c})^{1/2})$ with $A$ being a constant independent of temperature. At the transition point, $\chi_{\mathrm{SC}}L^{-1.75}$ of different system sizes will cross each other since the $\xi$ goes to infinity.

In Fig. 2, we show the superfluid density $\rho_\mathrm{s}$ for different system sizes $L$ with $J_z = J_\perp = 4U/3$. The size dependence of the superfluid density is weak in most cases, and we can fit the results to the following equation:

$$T_\mathrm{c}(L) = T_\mathrm{c} + \frac{a}{(\ln bL)^2}. \tag{12}$$

Below, we estimate $T_\mathrm{c}$ by these extrapolations.

To check the validity of these results obtained from $\rho_\mathrm{s}$, we also examine the superconducting pairing susceptibility for different system sizes, and the results are shown in Fig. 3. The superconducting transition temperature $T_\mathrm{c}$ is determined by the crossing point of the curves for different system sizes. The crossing point between the $L = 10$ and $L = 12$ curves is close to the $T_\mathrm{c}$ obtained from the superfluid density $\rho_\mathrm{s}$, confirming the validity of our results. However, statistical errors have a significant effect because the curves for different $L$ are close to each other, and finite-size effects also make it harder to extract $T_\mathrm{c}$. For these reasons, we prefer to use the superfluid density to estimate the superconducting transition temperature.

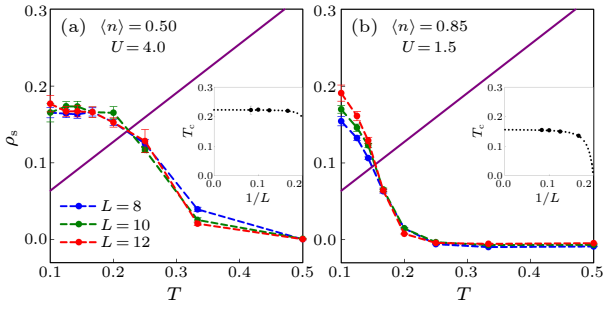


**Fig. 2.** Temperature dependence of the superfluid density $\rho_s$ with different lattice sizes at (a) $U = 4.0$ and $\langle n\rangle = 0.50$; (b) $U = 1.5$ and $\langle n\rangle = 0.85$. The straight line is $2T/\pi$, and the superfluid density $\rho_s$ intersects this straight line at $T_c$. Results are extrapolated to $L = \infty$ by fitting based on Eq. (12).

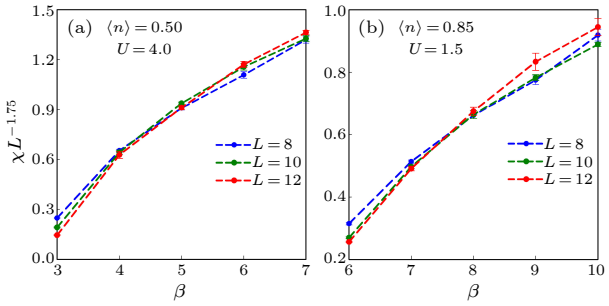


**Fig. 3.** Temperature dependence of superconducting pairing susceptibility with different lattice sizes at (a) $U = 4.0$ and $\langle n\rangle = 0.50$; (b) $U = 1.5$ and $\langle n\rangle = 0.85$. The values at different system sizes $L$ intersect each other at $T_c$.

Figure 1(b) shows $T_c$ as a function of electron filling from $U = 1.5$ to $U = 4.0$. As $U$ increases, the optimal filling shifts to $\langle n\rangle = 0.5$, which is close to the occupation of the $d_{x^2-y^2}$ orbital in single-crystal LNO. Recalling the definition of our model, the interlayer spin-exchange interaction also increases when $U$ becomes larger. When $J$ is large, a shift of the superconducting dome towards smaller electron filling was found within the bilayer $t$–$J$ model,[55] and an optimal doping at $\langle n\rangle = 0.5$ was also suggested for the mixD+V model.[56,57] In our work, where $U$ is present, the situation becomes more complex. Although $J$ stabilizes the binding energy, the monotonic increase of $T_c$ with increasing $U$ is not unexpected. However, the behavior at large $\langle n\rangle$ is particularly noteworthy, as a non-monotonic dependence of $T_c$ on $U$ emerges under low doping conditions, specifically, $T_c$ initially increases, but further enhancement of $U$ eventually suppresses superconductivity. We will later demonstrate that this phenomenon arises from the competition between $U$ and $J$, and that $U$ is detrimental to superconductivity in the low-doping regime. Due to this intricate dependence on $U$, the optimal doping shifts toward $\langle n\rangle = 0.5$ as $U$ increases.

The phase diagram shown in Fig. 1(b) also demonstrates a possible strange-metal-like behavior exhibited by this model. A superconducting dome as a function of doping arises in the bilayer model, which is similar to that in doped cuprates and exhibits precise scaling laws among the superconducting transition temperature, doping, and the linear-in-$T$ scattering coefficient.[58] The strange-metal-like behavior has also been reported in $La_3Ni_2O_{6.93}$[59] and LNO crystals.[13] We shall discuss this further along with the behavior of the regular part of resistivity later.

To investigate the superconducting transition temperature for decreasing $U$, we must activate the other three terms $g_0$, $g_4$, and $g_5$, to keep the system sign-problem-free. In Fig. 4, we demonstrate the behavior of superfluid density at $L = 12$ for different values of $U$ while keeping $J = 4.0$ fixed. Here, we can observe the varying dependence of $T_c$ on $U$. At low doping levels, $U$ could suppress $T_c$ when $J$ is fixed, and superconductivity might be influenced by other intertwined orders favored by $U$. This reveals an intrinsic constraint on improving $T_c$, and also indicates that higher doping, near $\langle n\rangle = 0.5$, is more beneficial for interlayer superconductivity. In LNO, since the interlayer spin-exchange originates from interlayer hopping and $U$, the effect of $U$ could be very significant.

We now turn off the $g_0$, $g_4$, and $g_5$ terms and investigate the effects of the $t_\perp$ term. In LNO, $t_\perp$ modifies the Fermi surface topology.[60] The interlayer hopping strengths for the $d_{x^2-y^2}$ and $d_{z^2}$ orbitals are different,[35,36] with that for the $d_{x^2-y^2}$ orbital being much smaller than that for the $d_{z^2}$ orbital. As we can see in Fig. 5, interlayer hopping adversely affects superconductivity in our model with fixed values of $U$ and $J$. This could be because $t_\perp$ favors bonding and antibonding states, while a large $t_\perp$ pushes these states away from the Fermi surface, thereby suppressing many-body effects. In fact, the strength of $t_\perp$ for the $d_{z^2}$ orbital can reach a ratio of $t_\perp/t > 5$, a regime which is examined in Fig. 5.

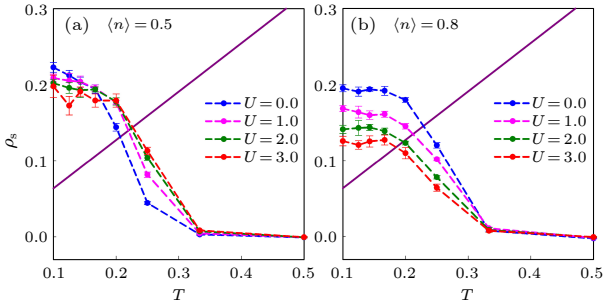


**Fig. 4.** Temperature dependence of the superfluid density $\rho_s$ at different $U$ with $L = 12$ and $J_z = J_\perp = 4.0$ for (a) $\langle n\rangle = 0.5$ and (b) $\langle n\rangle = 0.8$. Unlike other parts of this work, the relation $J = 4U/3$ does not hold in this diagram to maintain the sign-problem-free condition.

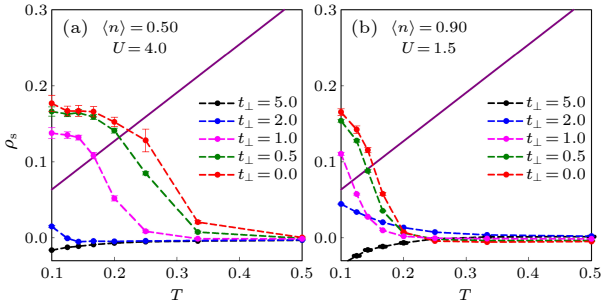


**Fig. 5.** Temperature dependence of the superfluid density $\rho_s$ with fixed $L = 12$ and different $t_\perp$ at (a) $U = 4.0$ and $\langle n\rangle = 0.5$; (b) $U = 1.5$ and $\langle n\rangle = 0.9$. $T_c$ is suppressed as $t_\perp$ increases.

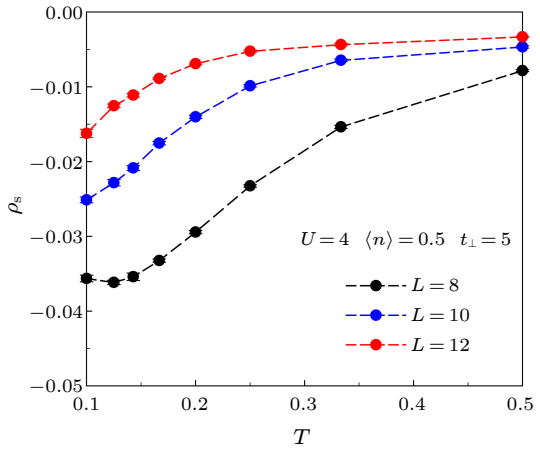


**Fig. 6.** Temperature dependence of the superfluid density $\rho_s$ with the large $t_\perp = 5$ and different $L$ at $U = 4.0$, $\langle n\rangle = 0.5$.

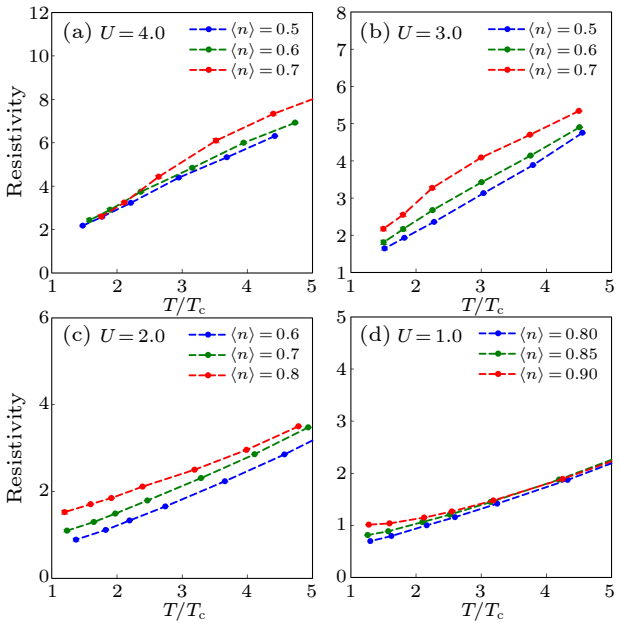


**Fig. 7.** Temperature dependence of the resistivity with $L = 12$ at (a) $U = 4.0$ and (b) $U = 1.5$. The resistivity shows a linear dependence on $T$ at relatively high temperatures.

We compare superfluid density $\rho_s$ with various $t_\perp$, and $T_c$ can be estimated by finding the crossing point of the $\rho_s$ curve and the line $2T/\pi$. One can see that a large $t_\perp$ does not favor superconductivity. In Fig. 5, when $t_\perp = 5.0$, the superfluid density drops below zero, which is unphysical at first glance. However, in calculating the limiting longitudinal and transverse responses, we use the smallest available momentum instead of taking the limit as the momentum approaches zero. This leads to errors in the results caused by finite-size effects. As seen in Fig. 6, the superfluid density gradually approaches zero as system size increases.

However, in the simulations above, we have fixed the strength of interactions $J$ and $U$. In real materials, the model parameters could be more complicated. The interlayer spin-exchange term $J$ originates from $U$ and $t_\perp$, and increasing $t_\perp$ will also enhance $J$. This is different from our model where the proportion of $U$ and $J$ is fixed. In real LNO systems, a moderate $t_\perp$ is beneficial to superconductivity, while a further increase in $t_\perp$ is detrimental to it.

In the studies of high-$T_c$ superconductors, strange-metal behavior which develops in the normal state is of great importance for theoretical understanding. As we can calculate current–current correlations to determine the superfluid density, it is straightforward to extract the regular part of the resistivity $R^{\rm reg}$ using the relation shown in Eq. (10). In Fig. 7, we show the resistivity at relatively high temperatures as the method we used is only compatible with the normal state. From this figure, a linear relationship between temperature $T$ and resistivity can be observed, and this relationship is clearer at lower electron densities $\langle n\rangle$. This may indicate a strange-metal behavior at relatively high temperatures, which has been widely observed in doped cuprates[58] and high-$T_c$ nickelate superconductors.[13,59] However, it should be noted that the regular part of the resistivity $R^{\rm reg}$ may be numerically shaped by the specific form of the equation, especially in imaginary-time calculations based on the high-temperature data. Thus, we only suggest the possibility of strange metallicity in the bilayer model; more evidence is necessary to confirm the strange metallicity, which exceeds the scope of this work.

*4. Conclusions.* We study a sign-problem-free bilayer Hubbard-like model using the DQMC algorithm, which is closely related to the recently discovered bilayer nickelate superconductor LNO. Both the promising reduced model for LNO and our model emphasize the significant role of the spin-exchange $J$ term in the formation of superconductivity. Moreover, due to the special symmetry of our model, we can avoid the sign problem in simulations at arbitrary electron fillings, allowing us to conduct DQMC simulations at relatively low temperatures with sufficient accuracy. Our unbiased numerical calculations show that optimal doping shifts toward $\langle n\rangle = 0.5$ as the interaction strength increases. In fact, this reflects a complex dependence on $U$: it enhances superconductivity at high doping but weakens it at low doping. The interlayer hopping term also weakens superconductivity. Furthermore, the regular part of the resistivity exhibits linear-temperature-dependent behavior, suggesting the possibility of strange metallicity. However, due to the limitations in both equation and method, the strange metallicity needs further confirmation.

*Acknowledgements.* This work was supported by the National Natural Science Foundation of China (Grant Nos. 12234016, 12174317 for C. Wu, and 12474218 for R. Ma, Z. Fan, and T. Ma), Beijing Natural Science Foundation (Grant No. 1242022 for R. Ma, Z. Fan, and T. Ma), and the New Cornerstone Science Foundation.

# References

[1] Wu M K, Ashburn J R, Torng C J, Hor P H, Meng R L, Gao L, Huang Z J, Wang Y Q, and Chu C W 1987 *Phys. Rev. Lett.* **58** 908
[2] Bednorz J G and Müller K A 1986 *Z. Phys. B* **64** 189

[3] Luo X, Chen H, Li Y, Gao Q, Yin C, Yan H, Miao T, Luo H, Shu Y, Chen Y, Lin C, Zhang S, Wang Z, Zhang F, Yang F, Peng Q, Liu G, Zhao L, Xu Z, Xiang T, and Zhou X J 2023 *Nat. Phys.* **19** 1841
[4] Yamamoto A, Takeshita N, Terakura C, and Tokura Y 2015 *Nat. Commun.* **6** 8990
[5] Chen X J, Struzhkin V V, Yu Y, Goncharov A F, Lin C T, Mao H K, and Hemley R J 2010 *Nature* **466** 950
[6] Kamihara Y, Watanabe T, Hirano M, and Hosono H 2008 *J. Am. Chem. Soc.* **130** 3296
[7] Yi M, Zhang Y, Shen Z X, and Lu D 2017 *npj Quantum Mater.* **2** 57
[8] Kuo H H, Chu J H, Palmstrom J C, Kivelson S A, and Fisher I R 2016 *Science* **352** 958
[9] Johnston D C 2010 *Adv. Phys.* **59** 803
[10] Paglione J and Greene R L 2010 *Nat. Phys.* **6** 645
[11] Stewart G R 2011 *Rev. Mod. Phys.* **83** 1589
[12] Li D, Lee K, Wang B Y, Osada M, Crossley S, Lee H R, Cui Y, Hikita Y, and Hwang H Y 2019 *Nature* **572** 624
[13] Sun H, Huo M, Hu X, Li J, Liu Z, Han Y, Tang L, Mao Z, Yang P, Wang B, Cheng J, Yao D X, Zhang G M, and Wang M 2023 *Nature* **621** 493
[14] Arovas D P, Berg E, Kivelson S A, and Raghu S 2022 *Annu. Rev. Condens. Matter Phys.* **13** 239
[15] Xu H, Chung C M, Qin M, Schollwöck U, White S R, and Zhang S 2024 *Science* **384** eadh7691
[16] Zheng B X, Chung C M, Corboz P, Ehlers G, Qin M P, Noack R M, Shi H, White S R, Zhang S, and Chan G K L 2017 *Science* **358** 1155
[17] Raghu S, Kivelson S A, and Scalapino D J 2010 *Phys. Rev. B* **81** 224505
[18] Qin Q and Yang Y F 2025 *npj Quantum Mater.* **10** 13
[19] Qin Q and Yang Y F 2023 *Phys. Rev. B* **108** L140504
[20] Qin Q, Wang J, and Yang Y F 2024 *Innov. Mater.* **2** 100102
[21] Qin M, Schäfer T, Andergassen S, Corboz P, and Gull E 2022 *Annu. Rev. Condens. Matter Phys.* **13** 275
[22] LeBlanc J P F, Antipov A E, Becca F, Bulik I W, Chan G K L, Chung C M, Deng Y, Ferrero M, Henderson T M, Jiménez-Hoyos C A, Kozik E, Liu X W, Millis A J, Prokof'ev N V, Qin M, Scuseria G E, Shi H, Svistunov B V, Tocchio L F, Tupitsyn I S, White S R, Zhang S, Zheng B X, Zhu Z, and Gull E 2015 *Phys. Rev. X* **5** 041041
[23] Schäfer T, Wentzell N, Šimkovic F, He Y Y, Hille C, Klett M, Eckhardt C J, Arzhang B, Harkov V, Le Régent F M, Kirsch A, Wang Y, Kim A J, Kozik E, Stepanov E A, Kauch A, Andergassen S, Hansmann P, Rohe D, Vik Y M, LeBlanc J P F, Zhang S, Tremblay A M S, Ferrero M, Parcollet O, and Georges A 2021 *Phys. Rev. X* **11** 011058
[24] Wu C, Hu J P, and Zhang S C 2003 *Phys. Rev. Lett.* **91** 186402
[25] Ma T, Wang D, and Wu C 2022 *Phys. Rev. B* **106** 054510
[26] Ma R and Ma T 2023 *Phys. Rev. B* **107** 214509
[27] Prasad Y, Medhi A, and Shenoy V B 2014 *Phys. Rev. A* **89** 043605
[28] Prasad Y 2022 *Phys. Rev. B* **106** 184506
[29] Prasad Y and Lee H 2024 *Phys. Rev. B* **109** 064506
[30] Osada M, Wang B Y, Lee K, Li D, and Hwang H Y 2020 *Phys. Rev. Mater.* **4** 121801
[31] Zeng S, Tang C S, Yin X, Li C, Li M, Huang Z, Hu J, Liu W, Omar G J, Jani H, Lim Z S, Han K, Wan D, Yang P, Pennycook S J, Wee A T S, and Ariando A 2020 *Phys. Rev. Lett.* **125** 147003
[32] Zeng S, Li C, Chow L E, Cao Y, Zhang Z, Tang C S, Yin X, Lim Z S, Hu J, Yang P, and Ariando A 2022 *Sci. Adv.* **8** eabl9927
[33] Liu Z, Sun H, Huo M, Ma X, Ji Y, Yi E, Li L, Liu H, Yu J, Zhang Z, Chen Z, Liang F, Dong H, Guo H, Zhong D, Shen B, Li S, and Wang M 2022 *Sci. China Phys. Mech. Astron.* **66** 217411
[34] Zhang Y, Su D, Huang Y, Shan Z, Sun H, Huo M, Ye K, Zhang J, Yang Z, Xu Y, Su Y, Li R, Smidman M, Wang M, Jiao L, and Yuan H 2024 *Nat. Phys.* **20** 1269
[35] Gu Y, Le C, Yang Z, Wu X, and Hu J 2023 arXiv:2306.07275 [cond-mat.supr-con]
[36] Luo Z, Hu X, Wang M, Wú W, and Yao D X 2023 *Phys. Rev. Lett.* **131** 126001
[37] Yang Y F, Zhang G M, and Zhang F C 2023 *Phys. Rev. B* **108** L201108
[38] Lu C, Pan Z, Yang F, and Wu C 2024 *Phys. Rev. Lett.* **132** 146002
[39] Kaneko T, Sakakibara H, Ochi M, and Kuroki K 2024 *Phys. Rev. B* **109** 045154
[40] Qu X Z, Qu D W, Chen J, Wu C, Yang F, Li W, and Su G 2024 *Phys. Rev. Lett.* **132** 036502
[41] Lechermann F, Gondolf J, Bötzel S, and Eremin I M 2023 *Phys. Rev. B* **108** L201121
[42] Jiang K, Wang Z, and Zhang F C 2024 *Chin. Phys. Lett.* **41** 017402
[43] Fan Z, Zhang J F, Zhan B, Lv D, Jiang X Y, Normand B, and Xiang T 2024 *Phys. Rev. B* **110** 024514
[44] Wu C and Zhang S C 2005 *Phys. Rev. B* **71** 155115
[45] Schlömer H, Schollwöck U, Grusdt F, and Bohrdt A 2023 arXiv:2311.03349 [cond-mat.str-el]
[46] Assaad F F and Evertz H G 2008 *Computational Many-Particle Physics* (Springer) p. 277
[47] White S R, Scalapino D J, Sugar R L, Loh E Y, Gubernatis J E, and Scalettar R T 1989 *Phys. Rev. B* **40** 506
[48] Scalapino D J, White S R, and Zhang S C 1992 *Phys. Rev. Lett.* **68** 2830
[49] Scalapino D J, White S R, and Zhang S 1993 *Phys. Rev. B* **47** 7995
[50] Fontenele R A, Costa N C, dos Santos R R, and Paiva T 2022 *Phys. Rev. B* **105** 184502
[51] Nelson D R and Kosterlitz J M 1977 *Phys. Rev. Lett.* **39** 1201
[52] Huang E W, Sheppard R, Moritz B, and Devereaux T P 2019 *Science* **366** 987
[53] Li Z X, Louie S G, and Lee D H 2023 *Phys. Rev. B* **107** L041103
[54] Li T and Yang J 2023 arXiv:2104.08733 [cond-mat.str-el]
[55] Chen J, Yang F, and Li W 2024 *Phys. Rev. B* **110** L041111
[56] Lange H, Homeier L, Demler E, Schollwöck U, Bohrdt A, and Grusdt F 2023 arXiv:2309.13040 [cond-mat.str-el]
[57] Lange H, Homeier L, Demler E, Schollwöck U, Grusdt F, and Bohrdt A 2024 *Phys. Rev. B* **109** 045127
[58] Yuan J, Chen Q, Jiang K, Feng Z, Lin Z, Yu H, He G, Zhang J, Jiang X, Zhang X, Shi Y, Zhang Y, Qin M, Cheng Z G, Tamura N, Yang Y F, Xiang T, Hu J, Takeuchi I, Jin K, and Zhao Z 2022 *Nature* **602** 431
[59] Wang G, Wang N N, Shen X L, Hou J, Ma L, Shi L F, Ren Z A, Gu Y D, Ma H M, Yang P T, Liu Z Y, Guo H Z, Sun J P, Zhang G M, Calder S, Yan J Q, Wang B S, Uwatoko Y, and Cheng J G 2024 *Phys. Rev. X* **14** 011040
[60] Ryee S, Witt N, and Wehling T O 2024 arXiv:2310.17465 [cond-mat.supr-con]